THE JOURNAL OF PHYSICAL CHEMISTRY LETTERS
A JOURNAL OF THE AMERICAN CHEMICAL SOCIETY

pubs.acs.org/JPCL

Letter

Pathway toward Optical Cycling and Laser Cooling of Functionalized Arenes

Debayan Mitra,* Zack D. Lasner, Guo-Zhu Zhu, Claire E. Dickerson, Benjamin L. Augenbraun, Austin D. Bailey, Anastassia N. Alexandrova, Wesley C. Campbell, Justin R. Caram, Eric R. Hudson, and John M. Doyle

Cite This: *J. Phys. Chem. Lett.* 2022, 13, 7029−7035

Read Online

ACCESS | Metrics & More | Article Recommendations | Supporting Information

ABSTRACT: Rapid and repeated photon cycling has enabled precision metrology and the development of quantum information systems using atoms and simple molecules. Extending optical cycling to structurally complex molecules would provide new capabilities in these areas, as well as in ultracold chemistry. Increased molecular complexity, however, makes realizing closed optical transitions more difficult. Building on already established strong optical cycling of diatomic, linear triatomic, and symmetric top molecules, recent work has pointed the way to cycling of larger molecules, including phenoxides. The paradigm for these systems is an optical cycling center bonded to a molecular ligand. Theory has suggested that cycling may be extended to even larger ligands, like naphthalene, pyrene, and coronene. Herein, we study optical excitation and fluorescent vibrational branching of CaO-□□, SrO-□□, and CaO-□ and find only weak decay to excited vibrational states, indicating a promising path to full quantum control and laser cooling of large arene-based molecules.

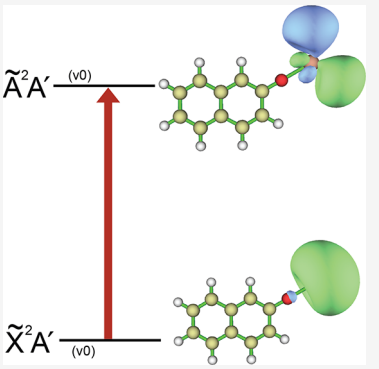

The repeated absorption and emission of photons by atoms is the fundamental process that underlies many advances in atomic, molecular, and optical science (AMO). This optical cycling enables the technique of laser cooling, as used for the deceleration of atoms emanating from a hot oven,[1] and magneto-optical trapping.[2] It is further employed for quantum state preparation and readout,[3−5] which enable ultraprecise clocks,[6−8] atom-based quantum simulators and computers,[9−11] and studies of single-quantum-state-controlled ultracold chemistry.[12−14]

Extending optical cycling to a wide variety of molecules is expected to bring a wealth of new science arising from their rotational and vibrational states. However, the complexity of molecules, as compared to atoms, brings new challenges for optical cycling. In particular, a molecule that is optically driven by a narrow band laser to an excited electronic state can decay to excited rotational and vibrational states in the electronic ground state. Thus, the molecule can end up in "dark" states that are no longer excited by the laser. Despite the difficulties of these dark state processes (i.e., "leakage" to excited rovibrational states), optical cycling and laser cooling of molecules has been accomplished by making use of symmetry-driven selection rules and multiwavelength laser excitation to "repump" rotational and vibrational dark states.[15] The diatomic molecules SrF,[16] CaF,[17,18] and YO[19] were the first molecules to be directly laser-cooled using this approach.

During the development of laser cooling of diatomic molecules, experimental work toward laser cooling of polyatomic molecules began with SrOH.[20] Soon after, it was proposed that low leakage to excited vibrational states (i.e., diagonal Franck−Condon factors) could be obtained in a class of alkaline earth (I) "metal-oxide-radical" polyatomic molecules, of which SrOH is an example.[21] The general concept of the use of nonbonding orbitals for quasi-closed transitions in polyatomic molecules was also proposed.[22] Since then, laser cooling has been successfully demonstrated in the linear triatomic molecules SrOH,[23] CaOH,[24,25] and YbOH[26] and the symmetric top molecule $CaOCH_3$.[27] Recently, CaOH was laser-cooled to temperatures <1 mK and confined in a MOT by repumping only nine vibrational loss channels (scattering $\sim 10^4$ photons).[25,28]

Two features of these molecular systems allow for successful optical cycling. First, alkaline-earth(-like) metals (such as Ca, Sr, or Yb) act as an optical cycling center (OCC) that is bonded to an electronegative ligand. Second, and relatedly, there are sufficiently few vibrational loss channels that repumping is technologically feasible.[29−31] The ionic bond between the metal atom and the ligand leads to a localized orbital of the valence electron near the metal atom.[32] Hence,

Received: May 11, 2022
Accepted: May 23, 2022
Published: July 28, 2022

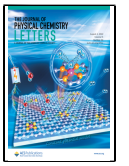

https://doi.org/10.1021/acs.jpclett.2c01430
J. Phys. Chem. Lett. 2022, 13, 7029−7035

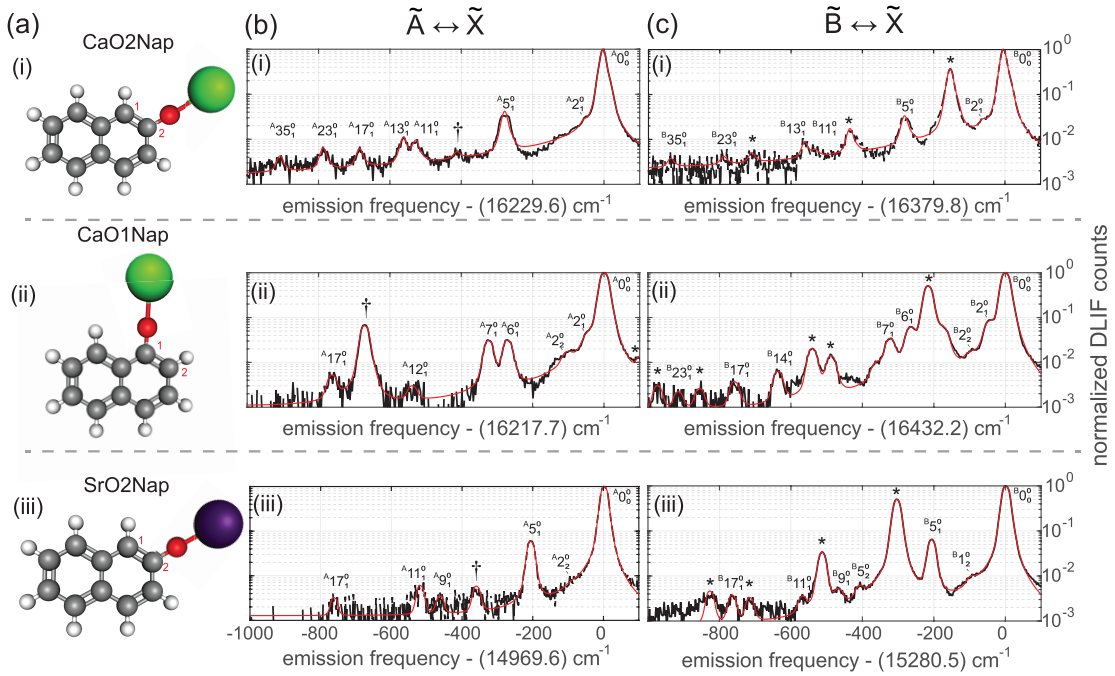

Figure 1. DLIF spectra of molecules studied in this work. Panels a(i–iii) are ball-and-stick representations of CaO2Nap, CaO1Nap, and SrO2Nap, respectively. White spheres denote hydrogen, gray denote carbon, red denote oxygen, green denote calcium, and purple denote strontium atoms. Also labeled are the only two distinguishable carbon bonding sites in naphthalene (1 and 2). Panels b(i–iii) are DLIF spectra after exciting the $\tilde{A} \leftarrow \tilde{X}$ transition for the molecular species a(i–iii) normalized to the peak height at 0 cm^{-1}. Black lines are experimental data that result from averaging ∼5000 repetitions. Panels c(i–iii) are $\tilde{B} \leftarrow \tilde{X}$ excitations. All attributed peaks have been labeled as ${}^{S}\nu_{f}^{i}$, where the first superscript defines the excited state ($\tilde{A}$ or $\tilde{B}$), the number ν denotes the ν^{th} vibrational mode, the second superscript i defines the vibrational quantum number in the excited state (always the vibrational ground state ($\nu = 0$) in the $\tilde{A}$ or $\tilde{B}$ state), and the subscript f is the vibrational quantum number in the ground $\tilde{X}$ state that the molecule decays to. Red lines represent fits to the DLIF spectra used to extract the VBRs for each decay pathway. Peaks marked with † represent contaminant peaks that cannot be ascribed to theoretically estimated harmonic modes or the overtones of the molecule of interest. The peaks marked with * are due to collision-induced transitions between the $\tilde{B}$ and the $\tilde{A}$ states. The peaks marked * and † have been excluded from VBR estimation.

when this electron is excited, it only weakly couples to bond stretching.

Building from the above principles and approaches, it was recently shown theoretically that an alkaline earth(I)-oxide unit attached to an electron-withdrawing ligand often led to a lone, metal-centered optically active electron.[33−35] This electron's orbital and environment is then qualitatively similar to those present in previously laser-cooled molecules, and therefore, strong optical cycling can be expected. Further, the theoretical calculations suggested that increasing the electron-withdrawing strength of the ligand by substitutions in the ligand could improve optical cycling performance. Some of these concepts were recently demonstrated for ligands composed of phenyl and its derivatives,[36] where it was suggested that the alkaline earth oxide unit could be considered a quantum functional group that could be used to gain control of larger molecules and provide a generic qubit moiety for attaching to large molecules and perhaps surfaces.

It is a tantalizing question whether even larger arenes would possess favorable properties for optical cycling. This idea was theoretically explored in ref 37, which found that larger rings in polycyclic aromatic molecules begin to close the highest occupied–lowest unoccupied molecular orbital (HOMO–LUMO) gap of the ligands relative to the electronic transition of the OCC. As the orbitals belonging to the arenes get closer in energy to the otherwise isolated electronic transition, they distort the potential energy surface and disrupt the vibrational overlap between electronic states. Therefore, as the number of rings is increased, the optical transition is expected to become progressively less diagonal. However, even in this case it may be possible to use an electron-withdrawing substitution around the ring to increase Franck–Condon diagonality. It was predicted that for ≥10 rings (ovalene), the HOMO–LUMO gap will be closed to the point that the transition would cease to be diagonal.[37]

Herein, we take the first step toward understanding the functionalization of large polycyclic arenes with an optical cycling center, which can act as a quantum functional group. We report on the production and spectroscopic study of CaO and SrO substituted naphthyl (Nap), measuring the optical decay to vibrational states of the ground electronic state. We present a solid-precursor-based production technique, which could be generalized to produce a large variety of arenes in a CBGB. Using this molecule source and the dispersed laser-induced fluorescence (DLIF) technique,[38−41] we detect and characterize the optical excitation and decay of naphthol-based molecules. We measure vibrational branching ratios (VBRs), which quantify the probability of decay from an excited electronic state to each vibrational state of the ground electronic manifold and serve as a measure of the ability to scatter a large number of photons. We observe that the molecule CaO-□–□ has a VBR for the vibrationless transition of 96(1)%. We also compare the isomers CaO-□–□ and CaO-□ and observe that for the latter, the transition becomes less

https://doi.org/10.1021/acs.jpclett.2c01430
J. Phys. Chem. Lett. 2022, 13, 7029−7035

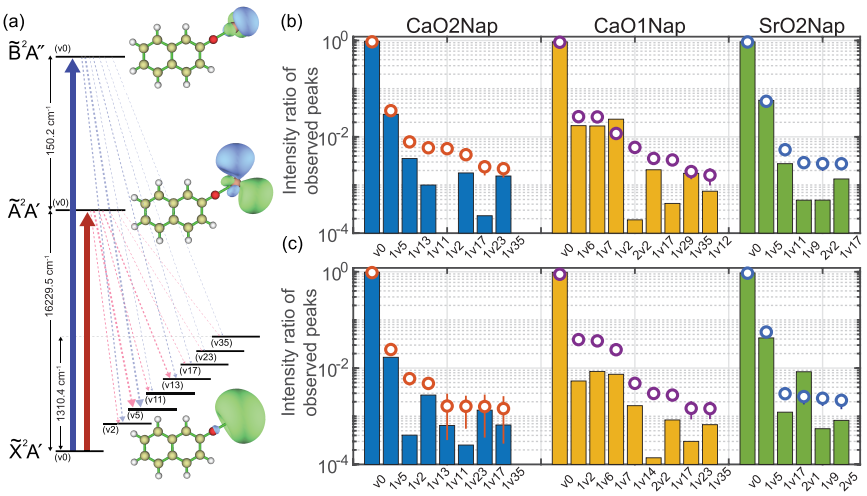

Figure 2. Energy level diagram and intensity ratios of all observed peaks for the three molecular species studied in this work and their comparison with theory. (a) Electronic energy levels ($\tilde{X}$, $\tilde{A}$, and $\tilde{B}$) and vibrational energy levels (v0 to v35) for CaO2Nap. Solid arrows indicate OPO excitation wavelengths. Dashed lines represent decays to vibrationally excited states (spacings are not to scale). Adjacent to the energy levels are MO representations of the ground ($\tilde{X}$) and both excited $\tilde{A}$ (in-plane) and $\tilde{B}$ (out-of-plane) states. (b) Intensity ratio of all observed peaks for $\tilde{A} \rightarrow \tilde{X}$ decay and (c) $\tilde{B} \rightarrow \tilde{X}$ decay. Vibrational modes are denoted as vM for the M^{th} vibrational mode, and NvM implies that N vibrational quanta are excited. Molecules are, from left to right: CaO2Nap, CaO1Nap, and SrO2Nap. Circles denote experimental intensity, while bars are from theory. Error bars are statistical standard errors from fits.

diagonal. Finally, we also perform spectroscopy on SrO-□-□ and find it also to be favorable for optical cycling.

Details of the experimental setup are provided in the Supporting Information.[42] Briefly, molecules are produced in a CBGB source via ablation of a solid precursor consisting of CaH_2 or SrH_2 powder mixed with 1-naphthol or 2-naphthol powder. The molecules are cooled by the buffer gas and are optically excited with a pulsed laser (OPO). The dispersed fluorescence spectrum is obtained by collecting molecular fluorescence light through a spectrometer onto a camera.

The four lowest-energy states of the molecules studied in this work can be represented as $\tilde{X}^2A'$, $\tilde{A}^2A'$, $\tilde{B}^2A''$ and $\tilde{C}^2A'$ in the C_s molecular symmetry group.[31] We explored the transitions between the ground vibrational state of the ground electronic state ($\tilde{X}$) and the ground vibrational state of the two lowest electronically excited manifolds ($\tilde{A}$ and $\tilde{B}$, Figure 2a). In the case of the $\tilde{A} \rightarrow \tilde{X}$ decay, we observe that the decay is predominantly to the ground-vibrational mode (denoted by $^{A}0_0^0$), with a small amount to the first Ca−O stretching mode $^{A}5_1^0$, for both CaO2Nap (Figure 1b(i)) and SrO2Nap (Figure 1b(iii)), and $^{A}6_1^0$ and $^{A}7_1^0$ for CaO1Nap (Figure 1b(ii)).

In the case of $\tilde{B} \rightarrow \tilde{X}$ decay, we observe similar behavior with the dominant decay to the ground vibrational mode ($^{B}0_0^0$). We also note that in every case, the excited molecules in the $\tilde{B}$ state can decay to the lower energy $\tilde{A}$ state via collisional relaxation. This process has been observed in similar experiments.[36,43,44] If a significant fraction of the molecules in the $\tilde{B}$ state decay via collisional relaxation, we expect to see not only the $^{A}0_1^0$ decay but also the higher $^{A}\nu_1^0$ vibrational decay peaks. Such collisional relaxation peaks are denoted with * in Figure 1c(i−iii). It is interesting to note that the reverse process of collisional excitation from $\tilde{A} \rightarrow \tilde{B}$ is also observed in the experiment, albeit at a much lower level than the $\tilde{B} \rightarrow \tilde{A}$ process. This is possibly due to energetic collision partners.

We fit the DLIF spectra to a series of Pearson distributions[42] and plot the result of the fitting in Figure 2b,c. In principle, a measurement of the VBRs requires knowledge of all vibrational modes, including any that may not be observed due to either insufficient measurement sensitivity, obstruction by spurious peaks, or because the corresponding decays lie outside of the detected range of wavelengths. Instead, we plot the ratio of the intensity of each observed peak to the sum of the intensities of all observed peaks. We plot this quantity for both experiment and density functional theory calculations for comparison (details can be found in the Supporting Information). The $\tilde{A} \rightarrow \tilde{X}$ (Figure 2b) and $\tilde{B} \rightarrow \tilde{X}$ (Figure 2c) decays show good agreement with theory for the dominant decay channels (0_0^0 for all three, 5_1^0 for MO2Nap, and 6_1^0 and 7_1^0 for CaO1Nap). Theory, however, fails to predict significant decay to the bending mode of the M−O-C bond (2_1^0) for MO2Nap. We speculate that this discrepancy is due to vibronic couplings among and anharmonicities within the low-frequency modes,[35,36,45,46] which are beyond the scope of the calculations presented in this work. However, our calculations predict a significant bending contribution for CaO1Nap for both the first (2_1^0) and second (2_2^0) harmonics (Figure 2). The contribution of the bending mode for CaO1Nap is by far the highest among all species examined here and the CaO-□-X molecules examined in ref 36. This is likely related to the fact that the CaO group in CaO1Nap is bonded to the carbon at position 1 of naphthalene (Figure 1a(ii)). This bonding site leads to a higher proximity to nearby carbon and hydrogen atoms and hence a greater mixing with the naphthol orbitals upon bending motion.[47]

In order to estimate the VBRs, we consider four systematic effects, as described in the Supporting Information. These include contributions of unobserved decays, population in vibrationally excited levels of $\tilde{X}$, fluctuations in excitation light power, and calibration of the spectrometer response. These sources of systematic uncertainty are added in quadrature with the statistical uncertainty of the fits to give upper and lower

https://doi.org/10.1021/acs.jpclett.2c01430
J. Phys. Chem. Lett. 2022, 13, 7029−7035

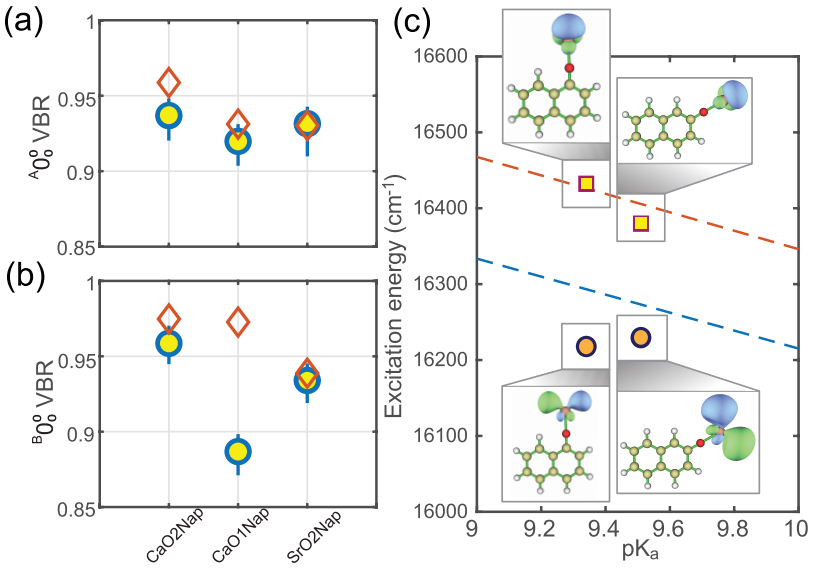

Figure 3. 0_0^0 VBR for the three molecules studied in this work and excitation energy as a function of pK_a. (a) primary VBR for the $\tilde{A}$ state ($^A0_0^0$) and (b) primary VBR for the $\tilde{B}$ state ($^B0_0^0$) for the three molecules, from left to right: CaO2Nap, CaO1Nap, and SrO2Nap. Experimental results (circles) are shown together with theory (diamonds). Error bars are a combination of statistical and systematic uncertainties. (c) $\tilde{X} \rightarrow \tilde{A}$ excitation energies are depicted as circles, and $\tilde{X} \rightarrow \tilde{B}$ excitation energies are depicted as squares for CaO1Nap (pK_a = 9.34) and CaO2Nap (pK_a = 9.51). Dashed line is excitation energy vs pK_a trend for CaOPh-X derivatives taken from ref 36. Insets are MO representation of each electronic state. $\tilde{B}$ state energies lie close to this trend line while $\tilde{A}$ state energies deviate significantly, likely due to in-plane orbitals in the $\tilde{A}$ state.

Table 1. Excitation Wavelength Relative to the Ground Vibrational ($\tilde{X}$) State (nm) and Measured Lifetime (ns) for the Nonvibrating $\tilde{A}$ and $\tilde{B}$ Electronic Excited States of the Three Molecules Measured in This Work[a]

Molecule	State	Excitation wavelength (nm)	Excitation energy (eV)	Lifetime (ns)
CaO-□	$\tilde{A}$	616.16(5)	2.012	19.8(2.5)
	$\tilde{B}$	610.51(5)	2.031	24.4(1.8)
CaO-⬡	$\tilde{A}$	616.61(5)	2.011	27.4(2.5)
	$\tilde{B}$	608.56(5)	2.037	22.4(2.4)
SrO-□	$\tilde{A}$	668.02(5)	1.856	28.5(2.8)
	$\tilde{B}$	654.43(5)	1.895	26.7(2.9)

[a]The uncertainty in wavelength estimation is the same for all measurements and is given by the spectral resolution (∼0.05 nm) of the optical spectrum analyzer used to measure the OPO center wavelength, which in turn was used to convert the camera pixels to wavelength. The lifetimes are obtained from exponential fits to the DLIF signals as a function of delay. The error bars are standard errors of fits.

uncertainty bounds for each vibronic decay in Table S1. We show the determined diagonal VBR for the $\tilde{A} \rightarrow \tilde{X}$ decay in Figure 3a and the $\tilde{B} \rightarrow \tilde{X}$ decay in Figure 3b, together with the theoretical predictions.

Our data elucidate the correlation between certain physical properties of calcium-based molecules with the electron-withdrawing property of the ligand. Naphthol can be compared with other proton donors based on their acid dissociation constant or pK_a. A smaller pK_a implies a more ionic O−H bond. We plot the excitation energies obtained for the $\tilde{A} \leftarrow \tilde{X}$ and $\tilde{B} \leftarrow \tilde{X}$ transitions for CaO1Nap and CaO2Nap as a function of pK_a of the corresponding naphthols in Figure 3c in comparison to the excitation energy trend for CaO-□ and derivatives obtained from ref 36. The $\tilde{B} \leftarrow \tilde{X}$ excitation energies closely follow the trend defined by the $\tilde{B} \leftarrow \tilde{X}$ transitions of the phenol derivatives. However, the $\tilde{A} \leftarrow \tilde{X}$ excitation energies deviate significantly from the trend. We attribute this effect to the fact that the $\tilde{B}$ state orbital is out-of-plane to the naphthalene rings while the $\tilde{A}$ state orbital is in-plane.[48] Because of the proximity with other carbon and hydrogen atoms, the bending force constant of the $\tilde{A}$ state can significantly deviate from a pure CaO-□-X bond (see Figure 3c insets).

Finally, in order to understand the potential for optical cycling and laser cooling, which is determined not only by the VBR, but also by the strength of the optical transition, we measure the lifetime of the $\tilde{A}$ and $\tilde{B}$ states. This is done by varying the delay between the OPO excitation and camera acquisition in steps of 5 ns (see Table 1). The lifetimes for all measured states are roughly 20−30 ns, similar to other molecules belonging to the CaOX family and compatible with maximum photon scattering rates of ∼10^6 s^{-1}.[24]

In conclusion, we demonstrate that a class of molecules based on a bicyclic aromatic compound, naphthalene, is favorable for optical cycling when functionalized with a calcium- or strontium-based optical cycling center. We

https://doi.org/10.1021/acs.jpclett.2c01430
J. Phys. Chem. Lett. 2022, 13, 7029−7035

establish a method that allows for the chemical formation of naphthol derivatives in a CBGB and could possibly be extended to larger arenes. Using DLIF spectroscopy, we measure that ∼96% of photon scattering events do not result in a change in the vibrational state of the molecule CaO-$\bar{C}_4\bar{H}_5$, which should allow for efficient optical cycling. We elucidate the role of geometry in decoupling the electronic and vibrational degrees of freedom by showing that the spatial proximity of the ligand in CaO-$\bar{C}_4\bar{H}_5$ causes a measurable decrease in 0_0^0 VBR and stronger excitation of other vibrational modes. The use of Sr (instead of Ca) might provide a technological advantage through the use of laser-diode-accessible transitions, while still providing a high 0_0^0 VBR (∼93%). Rotational closure for asymmetric top molecules is possible with 1−2 lasers per vibrational repump,[31] enabling rapid photon cycling. Optically enabled quantum state control of aromatic molecules could permit studies of chemical reactions via molecular collisions.[49,50] This work provides the stepping stone for the study of even larger aromatic compounds[37] or even surfaces[51] with quantum control over all degrees of freedom, opening new avenues in quantum chemistry. Finally, these measurements indicate that rapid photon cycling will be possible, which will enable laser cooling to the ultracold regime and fast and efficient quantum state manipulation of large arene molecules.

■ ASSOCIATED CONTENT

Supporting Information

The Supporting Information is available free of charge at https://pubs.acs.org/doi/10.1021/acs.jpclett.2c01430.

Technical details of the experimental setup, data acquisition, and fitting procedure; additional information on estimation of uncertainty and theoretical calculations along with Table S1 with all measured values (PDF)

■ AUTHOR INFORMATION

Corresponding Author

Debayan Mitra − *Department of Physics, Harvard University, Cambridge, Massachusetts 02138, United States; Harvard-MIT Center for Ultracold Atoms, Cambridge, Massachusetts 02138, United States;* Present Address: Department of Physics, Columbia University, New York, New York 10027, United States; orcid.org/0000-0002-2150-721X; Email: dm3710@columbia.edu

Authors

Zack D. Lasner − *Department of Physics, Harvard University, Cambridge, Massachusetts 02138, United States; Harvard-MIT Center for Ultracold Atoms, Cambridge, Massachusetts 02138, United States*

Guo-Zhu Zhu − *Department of Physics and Astronomy, University of California, Los Angeles, California 90095, United States; Center for Quantum Science and Engineering and Challenge Institute for Quantum Computation, University of California, Los Angeles, California 90095, United States;* orcid.org/0000-0002-5635-3679

Claire E. Dickerson − *Department of Chemistry and Biochemistry, University of California, Los Angeles, California 90095, United States*

Benjamin L. Augenbraun − *Department of Physics, Harvard University, Cambridge, Massachusetts 02138, United States; Harvard-MIT Center for Ultracold Atoms, Cambridge, Massachusetts 02138, United States;* orcid.org/0000-0003-4328-5176

Austin D. Bailey − *Department of Chemistry and Biochemistry, University of California, Los Angeles, California 90095, United States;* orcid.org/0000-0002-7278-6255

Anastassia N. Alexandrova − *Department of Chemistry and Biochemistry and Center for Quantum Science and Engineering, University of California, Los Angeles, California 90095, United States;* orcid.org/0000-0002-3003-1911

Wesley C. Campbell − *Department of Physics and Astronomy, University of California, Los Angeles, California 90095, United States; Center for Quantum Science and Engineering and Challenge Institute for Quantum Computation, University of California, Los Angeles, California 90095, United States*

Justin R. Caram − *Department of Chemistry and Biochemistry and Center for Quantum Science and Engineering, University of California, Los Angeles, California 90095, United States;* orcid.org/0000-0001-5126-3829

Eric R. Hudson − *Department of Physics and Astronomy, University of California, Los Angeles, California 90095, United States; Center for Quantum Science and Engineering and Challenge Institute for Quantum Computation, University of California, Los Angeles, California 90095, United States*

John M. Doyle − *Department of Physics, Harvard University, Cambridge, Massachusetts 02138, United States; Harvard-MIT Center for Ultracold Atoms, Cambridge, Massachusetts 02138, United States*

Complete contact information is available at: https://pubs.acs.org/10.1021/acs.jpclett.2c01430

Notes

The authors declare no competing financial interest.

■ ACKNOWLEDGMENTS

The authors thank Timothy C. Steimle for sharing critical equipment and for useful discussions. MO visualizations were performed using Multiwfn.[52] This work was supported by grants from the Keck Foundation, the CUA, the DOE, National Science Foundation (Grants No. PHY-1255526, No. PHY-1415560, No. PHY-1912555, No. CHE-1900555, and No. DGE-1650604), and Army Research Office (Grants No. W911NF-15-1-0121, No. W911NF-14-1-0378, No. W911NF-13-1-0213, and No. W911NF-17-1-0071) grants. C.E.D. acknowledges NSF GFRP Grant Nos. DGE-2034835 and 20223563.

■ REFERENCES

(1) Phillips, W. D.; Metcalf, H. Laser Deceleration of an Atomic Beam. *Phys. Rev. Lett.* **1982**, *48*, 596−599.

(2) Raab, E. L.; Prentiss, M.; Cable, A.; Chu, S.; Pritchard, D. E. Trapping of Neutral Sodium Atoms with Radiation Pressure. *Phys. Rev. Lett.* **1987**, *59*, 2631−2634.

(3) Bernien, H.; Schwartz, S.; Keesling, A.; Levine, H.; Omran, A.; Pichler, H.; Choi, S.; Zibrov, A. S.; Endres, M.; Greiner, M.; Vuletić, V.; Lukin, M. D. Probing Many-Body Dynamics on a 51-Atom Quantum Simulator. *Nature* **2017**, *551*, 579−584.

(4) Monroe, C.; Campbell, W. C.; Duan, L.-M.; Gong, Z.-X.; Gorshkov, A. V.; Hess, P.; Islam, R.; Kim, K.; Pagano, G.; Richerme, P.; Senko, C.; Yao, N. Y. Programmable Quantum Simulations of Spin Systems with Trapped Ions. *Rev. Mod. Phys.* **2021**, *93*, 025001.

(5) Morgado, M.; Whitlock, S. Quantum Simulation and Computing with Rydberg-Interacting Qubits. *AVS Quantum Sci.* **2021**, *3*, 023501.
(6) Young, A. W.; Eckner, W. J.; Milner, D.; William, R.; Kedar; Norcia, M. A.; Oelker, E.; Schine, N.; Ye, J.; Kaufman, A. M. Half-Minute-Scale Atomic Coherence and High Relative Stability in a Tweezer Clock. *Nature* **2020**, *588*, 408−413.
(7) Ohmae, N.; et al. Transportable Strontium Optical Lattice Clocks Operated Outside Laboratory at the Level of 10^{-18} Uncertainty. *Adv. Quantum Technol.* **2021**, *4*, 2100015.
(8) Brewer, S. M.; Chen, J.-S.; Hankin, A. M.; Clements, E. R.; Chou, C. W.; Wineland, D. J.; Hume, D. B.; Leibrandt, D. R. $^{27}Al^{+}$ Quantum-Logic Clock with a Systematic Uncertainty Below 10^{-18}. *Phys. Rev. Lett.* **2019**, *123*, 033201.
(9) Chiu, C. S.; Ji, G.; Bohrdt, A.; Xu, M.; Knap, M.; Demler, E.; Grusdt, F.; Greiner, M.; Greif, D. String Patterns in the Doped Hubbard Model. *Science* **2019**, *365*, 251−256.
(10) Semeghini, G.; et al. Probing Topological Spin Liquids on a Programmable Quantum Simulator. *Science* **2021**, *374*, 1242−1247.
(11) Grzesiak, N.; Blümel, R.; Wright, K.; Beck, K. M.; Pisenti, N. C.; Li, M.; Chaplin, V.; Amini, J. M.; Debnath, S.; Chen, J.-S.; Nam, Y. Efficient Arbitrary Simultaneously Entangling Gates on a Trapped-Ion Quantum Computer. *Nat. Commun.* **2020**, *11*, 2963.
(12) Balakrishnan, N. Perspective: Ultracold Molecules and the Dawn of Cold Controlled Chemistry. *J. Chem. Phys.* **2016**, *145*, 150901.
(13) Liu, Y.; Hu, M.-G.; Nichols, M. A.; Yang, D.; Xie, D.; Guo, H.; Ni, K.-K. Precision Test of Statistical Dynamics with State-to-State Ultracold Chemistry. *Nature* **2021**, *593*, 379−384.
(14) Heazlewood, B. R.; Softley, T. P. Towards Chemistry at Absolute Zero. *Nat. Rev. Chem.* **2021**, *5*, 125−140.
(15) McCarron, D. Laser Cooling and Trapping Molecules. *J. Phys. B: At. Mol. Opt. Phys.* **2018**, *51*, 212001.
(16) Shuman, E. S.; Barry, J. F.; DeMille, D. Laser Cooling of a Diatomic Molecule. *Nature* **2010**, *467*, 820−823.
(17) Truppe, S.; Williams, H.; Hambach, M.; Caldwell, L.; Fitch, N.; Hinds, E.; Sauer, B.; Tarbutt, M. Molecules Cooled Below the Doppler Limit. *Nat. Phys.* **2017**, *13*, 1173−1176.
(18) Anderegg, L.; Augenbraun, B. L.; Chae, E.; Hemmerling, B.; Hutzler, N. R.; Ravi, A.; Collopy, A.; Ye, J.; Ketterle, W.; Doyle, J. M. Radio Frequency Magneto-Optical Trapping of CaF with High Density. *Phys. Rev. Lett.* **2017**, *119*, 103201.
(19) Collopy, A. L.; Ding, S.; Wu, Y.; Finneran, I. A.; Anderegg, L.; Augenbraun, B. L.; Doyle, J. M.; Ye, J. 3D Magneto-Optical Trap of Yttrium Monoxide. *Phys. Rev. Lett.* **2018**, *121*, 213201.
(20) Kozyryev, I.; Baum, L.; Matsuda, K.; Olson, P.; Hemmerling, B.; Doyle, J. M. Collisional Relaxation of Vibrational States of SrOH with He at 2 K. *New J. Phys.* **2015**, *17*, 045003.
(21) Kozyryev, I.; Baum, L.; Matsuda, K.; Doyle, J. M. Proposal for Laser Cooling of Complex Polyatomic Molecules. *ChemPhysChem* **2016**, *17*, 3641−3648.
(22) Isaev, T. A.; Berger, R. Polyatomic Candidates for Cooling of Molecules with Lasers from Simple Theoretical Concepts. *Phys. Rev. Lett.* **2016**, *116*, 063006.
(23) Kozyryev, I.; Baum, L.; Matsuda, K.; Augenbraun, B. L.; Anderegg, L.; Sedlack, A. P.; Doyle, J. M. Sisyphus Laser Cooling of a Polyatomic Molecule. *Phys. Rev. Lett.* **2017**, *118*, 173201.
(24) Baum, L.; Vilas, N. B.; Hallas, C.; Augenbraun, B. L.; Raval, S.; Mitra, D.; Doyle, J. M. 1D Magneto-Optical Trap of Polyatomic Molecules. *Phys. Rev. Lett.* **2020**, *124*, 133201.
(25) Vilas, N. B.; Hallas, C.; Anderegg, L.; Robichaud, P.; Winnicki, A.; Mitra, D.; Doyle, J. M. Magneto-optical trapping and sub-Doppler cooling of a polyatomic molecule. *Nature* **2022**, *606*, 70−74.
(26) Augenbraun, B. L.; Lasner, Z. D.; Frenett, A.; Sawaoka, H.; Miller, C.; Steimle, T. C.; Doyle, J. M. Laser-Cooled Polyatomic Molecules for Improved Electron Electric Dipole Moment Searches. *New J. Phys.* **2020**, *22*, 022003.
(27) Mitra, D.; Vilas, N. B.; Hallas, C.; Anderegg, L.; Augenbraun, B. L.; Baum, L.; Miller, C.; Raval, S.; Doyle, J. M. Direct Laser Cooling of a Symmetric Top Molecule. *Science* **2020**, *369*, 1366−1369.
(28) Baum, L.; Vilas, N. B.; Hallas, C.; Augenbraun, B. L.; Raval, S.; Mitra, D.; Doyle, J. M. Establishing a Nearly Closed Cycling Transition in a Polyatomic Molecule. *Phys. Rev. A* **2021**, *103*, 043111.
(29) Rosa, M. D. Laser-Cooling Molecules. *Eur. Phys. J. D* **2004**, *31*, 395−402.
(30) Ivanov, M. V.; Bangerter, F. H.; Krylov, A. I. Towards a Rational Design of Laser-Coolable Molecules: Insights from Equation-of-Motion Coupled-Cluster Calculations. *Phys. Chem. Chem. Phys.* **2019**, *21*, 19447−19457.
(31) Augenbraun, B. L.; Doyle, J. M.; Zelevinsky, T.; Kozyryev, I. Molecular Asymmetry and Optical Cycling: Laser Cooling Asymmetric Top Molecules. *Phys. Rev. X* **2020**, *10*, 031022.
(32) Ellis, A. M. Main Group Metal-Ligand Interactions in Small Molecules: New Insights from Laser Spectroscopy. *Int. Rev. Phys. Chem.* **2001**, *20*, 551−590.
(33) Ivanov, M. V.; Bangerter, F. H.; Wójcik, P.; Krylov, A. I. Toward Ultracold Organic Chemistry: Prospects of Laser Cooling Large Organic Molecules. *J. Phys. Chem. Lett.* **2020**, *11*, 6670−6676.
(34) Ivanov, M. V.; Gulania, S.; Krylov, A. I. Two Cycling Centers in one Molecule: Communication by Through-Bond Interactions and Entanglement of the Unpaired Electrons. *J. Phys. Chem. Lett.* **2020**, *11*, 1297−1304.
(35) Dickerson, C. E.; Guo, H.; Shin, A. J.; Augenbraun, B. L.; Caram, J. R.; Campbell, W. C.; Alexandrova, A. N. Franck-Condon Tuning of Optical Cycling Centers by Organic Functionalization. *Phys. Rev. Lett.* **2021**, *126*, 123002.
(36) Zhu, G.; Mitra, D.; Augenbraun, B. L.; Dickerson, C. E.; Frim, M. J.; Lao, G.; Lasner, Z. D.; Alexandrova, A. N.; Campbell, W. C.; Caram, J. R.; Doyle, J. M.; Hudson, E. R. Functionalizing Aromatic Compounds with Optical Cycling Centers. *Nat. Chem.* **2022**, DOI: 10.1038/s41557-022-00998-x.
(37) Dickerson, C. E.; Guo, H.; Zhu, G.-Z.; Hudson, E. R.; Caram, J. R.; Campbell, W. C.; Alexandrova, A. N. Optical Cycling Functionalization of Arenes. *J. Phys. Chem. Lett.* **2021**, *12*, 3989−3995.
(38) Reilly, N. J.; Schmidt, T. W.; Kable, S. H. Two-Dimensional Fluorescence (Excitation/Emission) Spectroscopy as a Probe of Complex Chemical Environments. *J. Phys. Chem. A* **2006**, *110*, 12355−12359.
(39) Gascooke, J. R.; Alexander, U. N.; Lawrance, W. D. Two Dimensional Laser Induced Fluorescence Spectroscopy: A Powerful Technique for Elucidating Rovibronic Structure in Electronic Transitions of Polyatomic Molecules. *J. Chem. Phys.* **2011**, *134*, 184301.
(40) Kokkin, D. L.; Steimle, T. C.; DeMille, D. Branching Ratios and Radiative Lifetimes of the U, L, and I States of Thorium Oxide. *Phys. Rev. A* **2014**, *90*, 062503.
(41) Augenbraun, B. L.; Lasner, Z. D.; Frenett, A.; Sawaoka, H.; Le, A. T.; Doyle, J. M.; Steimle, T. C. Observation and Laser Spectroscopy of Ytterbium Monomethoxide, $YbOCH_3$. *Phys. Rev. A* **2021**, *103*, 022814.
(42) See the Supporting Information.
(43) Paul, A. C.; Sharma, K.; Reza, M. A.; Telfah, H.; Miller, T. A.; Liu, J. Laser-Induced Fluorescence and Dispersed-Fluorescence Spectroscopy of the $A^2E - X^2A_1$ Transition of Jet-Cooled Calcium Methoxide ($CaOCH_3$) Radicals. *J. Chem. Phys.* **2019**, *151*, 134303.
(44) Dagdigian, P. J. State-Resolved Collision-Induced Electronic Transitions. *Annu. Rev. Phys. Chem.* **1997**, *48*, 95−123.
(45) Domcke, W.; Cederbaum, L.; Köppel, H.; Von Niessen, W. A Comparison of Different Approaches to the Calculation of Franck-Condon Factors for Polyatomic Molecules. *Mol. Phys.* **1977**, *34*, 1759−1770.
(46) Fischer, G. *Vibronic Coupling: The Interaction between the Electronic and Nuclear Motions*; Academic Press, 1984.
(47) Radkowska, I.; Bragiel, P. 1-Naphthols as Components for Multifunctional Material Systems (MFMS): the Molecular Modeling Approach. *Struct. Chem.* **2021**, *32*, 259−273.

https://doi.org/10.1021/acs.jpclett.2c01430
J. Phys. Chem. Lett. 2022, 13, 7029−7035

(48) Morbi, Z.; Zhao, C.; Bernath, P. F. A high-resolution analysis of the $C^2A_1 - - X^2A_1$ transition of $CaNH_2$: Pure Precession in Polyatomic Molecules. *J. Chem. Phys.* **1997**, *106*, 4860−4868.
(49) Augustovičová, L. D.; Bohn, J. L. Ultracold Collisions of Polyatomic Molecules: CaOH. *New J. Phys.* **2019**, *21*, 103022.
(50) Cheuk, L. W.; Anderegg, L.; Bao, Y.; Burchesky, S.; Yu, S. S.; Ketterle, W.; Ni, K.-K.; Doyle, J. M. Observation of Collisions between Two Ultracold Ground-State CaF Molecules. *Phys. Rev. Lett.* **2020**, *125*, 043401.
(51) Guo, H.; Dickerson, C. E.; Shin, A. J.; Zhao, C.; Atallah, T. L.; Caram, J. R.; Campbell, W. C.; Alexandrova, A. N. Surface Chemical Trapping of Optical Cycling Centers. *Phys. Chem. Chem. Phys.* **2021**, *23*, 211−218.
(52) Lu, T.; Chen, F. Multiwfn: A Multifunctional Wavefunction Analyzer. *J. Comput. Chem.* **2012**, *33*, 580−592.

https://doi.org/10.1021/acs.jpclett.2c01430
J. Phys. Chem. Lett. 2022, 13, 7029−7035